THE JOURNAL OF BIOLOGICAL CHEMISTRY VOL. 288, NO. 4, pp. 2700–2710, January 25, 2013
Published in the U.S.A.

# Isolation and Characterization of RNA Polymerase *rpoB* Mutations That Alter Transcription Slippage during Elongation in *Escherichia coli*[*]

Received for publication, October 19, 2012 Published, JBC Papers in Press, December 5, 2012, DOI 10.1074/jbc.M112.429464

**Yan Ning Zhou[1], Lucyna Lubkowska[1], Monica Hui[2], Carolyn Court, Shuo Chen[3], Donald L. Court, Jeffrey Strathern, Ding Jun Jin[4], and Mikhail Kashlev[5]**

*From the Gene Regulation and Chromosome Biology Laboratory, National Cancer Institute, National Institutes of Health, Frederick National Laboratory for Cancer Research, Frederick, Maryland 21702*

**Background:** The domains in RNA polymerase involved in elongation slippage are unknown.
**Results:** We isolated *E. coli* RNA polymerase *rpoB* mutants with altered transcriptional slippage.
**Conclusion:** The fork domain of RNA polymerase controls slippage. Biochemical analysis of the mutants validates the genetic schemes.
**Significance:** Our work sheds light on the mechanism for maintenance of RNA-DNA register during transcription.

**Transcription fidelity is critical for maintaining the accurate flow of genetic information. The study of transcription fidelity has been limited because the intrinsic error rate of transcription is obscured by the higher error rate of translation, making identification of phenotypes associated with transcription infidelity challenging. Slippage of elongating RNA polymerase (RNAP) on homopolymeric A/T tracts in DNA represents a special type of transcription error leading to disruption of open reading frames in *Escherichia coli* mRNA. However, the regions in RNAP involved in elongation slippage and its molecular mechanism are unknown. We constructed an A/T tract that is out of frame relative to a downstream *lacZ* gene on the chromosome to examine transcriptional slippage during elongation. Further, we developed a genetic system that enabled us for the first time to isolate and characterize *E. coli* RNAP mutants with altered transcriptional slippage *in vivo*. We identified several amino acid residues in the β subunit of RNAP that affect slippage *in vivo* and *in vitro*. Interestingly, these highly clustered residues are located near the RNA strand of the RNA-DNA hybrid in the elongation complex. Our *E. coli* study complements an accompanying study of slippage by yeast RNAP II and provides the basis for future studies on the mechanism of transcription fidelity.**

*Escherichia coli* RNA polymerase (RNAP)[6] is a multisubunit enzyme that exists in two forms: holoenzyme ($\alpha_2\beta\beta'\omega\sigma$) and core enzyme ($\alpha_2\beta\beta'\omega$). The holoenzyme recognizes a promoter to initiate transcription. After initiation, $\sigma$ is released leaving core RNAP engaged in transcription elongation and subsequent termination (1, 2). Mutational analyses of RNAP have identified important regulatory regions in the enzyme affecting different steps in the transcription cycle (3). Regions in the large subunits of bacterial RNAP, $\beta$ and $\beta'$, form the active center of the enzyme and template/transcript binding sites (1). Residues in these regions are conserved in eukaryotic RNAP II (4), suggesting that the functions of RNAP are also conserved throughout evolution.

Transcription fidelity (5) is an important mechanism to ensure the accuracy of genetic information. Despite its importance, transcription fidelity is understudied, mainly because of the difficulties of identifying phenotypes associated with an increase in transcription errors (6), which are often masked by the much higher error rates in translation (7, 8). In this regard, earlier pioneering studies examining the effect of RNAP mutants on misreading of a point nonsense mutation during transcription (9, 10) have been complicated by the frequency of nontranscriptional errors induced under stress conditions (11). It becomes evident that new approaches that do not depend on the misreading of point mutations in a message are needed to study transcription fidelity. Two mutations in the largest Rpb1 subunit (the homolog of $\beta'$) of the yeast RNAP II were recently reported with a pronounced effect on transcription fidelity *in vivo* and *in vitro* (12, 13). The slow growth phenotype of the yeast Rpb1 fidelity mutants highlighted the potential importance of transcription fidelity for cell viability (12, 13). Point mutations D675Y in the $\beta$ subunit and N458D/S in the $\beta'$ subunit of *E. coli* RNAP that reduced fidelity *in vitro* were also described (14, 15). Rifampicin-resistant P564L mutation in the $\beta$ subunit (also known as *ack-1* (9)) was reported to decrease

* This work was supported, in whole or in part, by the National Institutes of Health Intramural Research Program. This work was also supported by the National Cancer Institute and the Center for Cancer Research.

[1] These authors contributed equally to this work.
[2] Present address: Dept. of Microbiology, New York University School of Medicine, New York, NY 10016.
[3] Present address: Medical School, University of Connecticut School of Medicine, Farmington, CT 06030.
[4] To whom correspondence may be addressed: Gene Regulation and Chromosome Biology Laboratory, Center for Cancer Research, National Cancer Institute, Frederick National Laboratory for Cancer Research, P.O. Box B, Frederick, MD 21702. Tel.: 301-846-7684; Fax: 301-846-1798; E-mail: jind@mail.nih.gov.
[5] To whom correspondence may be addressed: Gene Regulation and Chromosome Biology Laboratory, Center for Cancer Research, National Cancer Institute, Frederick National Laboratory for Cancer Research, P.O. Box B, Frederick, MD 21702. Tel.: 301-846-7684; Fax: 301-846-1798; E-mail: kashlevm@mail.nih.gov.

[6] The abbreviations used are: RNAP, RNA polymerase; nt, nucleotide(s); NTA, nitrilotriacetic acid; TEC, ternary elongation complex(es); MacLac, McConkey lactose.

**TABLE 1**
**Strains and plasmids used in the study**

| | Relevant genotype/comment | Source |
|---|---|---|
| **Strain** | | |
| MG1655 | Prototype *E. coli* K-12 strain | Carol Gross |
| CAG3002 | MG1655 *btuB*::Tn*10* linked to *rpoBC* | Ref. 48 |
| CAG3246 | MG1655 *recA56 srl*::Tn*10* | Ref. 48 |
| NY348 | *rpoC-his* tag fusion<>*kan* | Don Court |
| NC397 | *lacI′*<>*kan*<>*cat sacB*<>*lacZYA* harboring a defective λ *cI857* prophage for recombineering | Ref. 44 |
| MM111 | NC397 *lacI′*<>*spacer*<>*′lacZ* | This work |
| MH131A | MM111 *mhpR*::*cat*<>p*Tac***lacI′* | This work |
| Slippage strains | MG1655 *mhpR*::*cat*<>p*Tac***lacI′*<> *spacer*<>*′lacZ* | This work |
| **Plasmids** | | |
| pSim19 | Provides λ Red system; curable at ≥37 °C because of temperature-sensitive plasmid replication; spectomycin resistance | Don Court |
| pDJ853 | Constitutive expression of *rlpJL rpoB-his* | This work |

**TABLE 2**
**Chromosomal rpoB Rif$^R$ mutants used in the study**

| Strain | Amino acid change | Codon change | Source |
|---|---|---|---|
| CC256 | V146F | GTT → TTC | This work |
| CC257 | V146G | GTT → GGG | This work |
| CC258 | Q148H | CAG → CAC | This work |
| CC259 | Q148L | CAG → TTA | This work |
| CC262 | Q148K | CAG → AAA | This work |
| CC261 | Q148R | CAG → CGA | This work |
| CC148 | L511P | CTG → CCC | This work |
| CC141 | S512F | TCT → TTT | This work |
| CC143 | S512Y | TCT → TAC | This work |
| *rpoB3445* | Δ[G507-Q510] | Δ12 nt | Ref. 48 |
| *rpoB8* | Q513P | CAG → CCG | Ref. 48 |
| *rpoB101* | Q513L | CAG → CTG | Ref. 48 |
| CC264 | Q513C | CAG → TGT | This work |
| CC271 | Q513D | CAG → GAT | This work |
| *rpoB113* | D516N | GAC → AAC | Ref. 48 |
| *rpoB148* | D516V | GAC → GTC | Ref. 48 |
| CC144 | D516Y | GAC → TAT | This work |
| *rpoB3051* | [D516Q517]X2 | [GACCAG]X2 | Ref. 48 |
| CC140 | N518D | AAC → GAT | This work |
| *rpoB3595* | S522F | TCT → TTT | Ref. 48 |
| CC137 | S522Y | TCT → TAC | This work |
| CC117 | T525R | ACG → CGC | This work |
| *rpoB2* | H526Y | CAC → TAC | Ref. 48 |
| CC121 | H526L | CAC → CTT | This work |
| CC122 | H526N | CAC → AAT | This work |
| *rpoB3401* | R529C | CGT → TGT | Ref. 48 |
| CC253 | R529L | CGT → TTA | This work |
| CC254 | R529S | CGT → TCT | This work |
| *rif180* | R529H | CGT → CAT | Ref. 61 |
| *rpoB114* | S531F | TCC → TTC | Ref. 48 |
| CC124 | S531Y | TCC → TAT | This work |
| *rpoB3449* | ΔA532 | ΔGCA | Ref. 48 |
| CC125 | A532E | GCA → GAG | This work |
| *rpoB3443* | L533P | CTC → CCC | Ref. 48 |
| CC460 | L533H | CTC → CAT | This work |
| CC461 | L533R | CTC → CGA | This work |
| CC136 | G534A | GGC → GCA | This work |
| CC130 | G534S | GGC → AGT | This work |
| *rpoB3370* | T563P | ACC → CCC | Ref. 48 |
| *rpoB111* | P564L | CCT → CTT | Ref. 48 |
| CC276 | P564H | CCT → ATG | This work |
| CC463 | G570C | GGT → TGC | This work |
| CC464–116 | G570Q | GGT → CAA | This work |
| CC464–114 | G570M | GGT → ATG | This work |
| CC464–104 | G570A | GGT → GCA | This work |
| *rpoB7* | I572F | ATC → TTC | Ref. 48 |
| CC139 | I572N | ATC → AAT | This work |
| CC267 | I572K | ATC → AAA | This work |
| CC149 | I752T | ATC → ACA | This work |
| CC134 | S574F | TCT → TTC | This work |
| *rpoB3406* | R687H | CGT → CAT | Ref. 48 |

transcription fidelity *in vivo* and was recently shown to increase molecular noise in *E. coli* cells because of transient RNA errors (16).

There are two types of transcription mistakes: misincorporation of nucleotides and transcription slippage. The mechanism of transcription slippage is unknown, but its biological consequences are well documented (17–27). Slippage constitutes a temporary loss of DNA register by RNAP leading to insertions and deletions of nucleotides in mRNA (18, 19). It is proposed that accumulation of the mistranslated proteins derived from transcription slippage may be associated with human diseases and tumorigenesis, including Alzheimer disease, Down syndrome, and colorectal cancer (24, 28–31). Bacterial RNAP makes slippage products during both initiation (25, 26, 32, 33) and elongation (20, 22, 27, 34–36). Some of these slippage events are involved in gene regulation and bacterial pathogenesis. *E. coli* RNAP mutants in the *rpoB* gene encoding the β subunit that alter initiation at promoters containing a short run of A/T base pairs have been studied (37, 38); however, RNAP mutants that alter transcriptional slippage during elongation have not been identified. High efficiencies of transcription slippage on plasmid-borne DNA templates containing homopolymeric runs of 11A/T during elongation in *E. coli* cells (27) reveal a potential way to study transcription infidelity genetically.

In this study, we analyzed transcription slippage during elongation *in vivo* using a reporter gene in the *E. coli* chromosome and developed a genetic system to isolate and characterize RNAP *rpoB* mutants with altered transcriptional slippage phenotypes. Our study took advantage of genetic results from a yeast system used for studying slippage by RNAP II as described in the accompanying article (39). We identified a cluster of amino acid residues in RNAP encapsulating the RNA-DNA hybrid region that controls transcription slippage during elongation. Biochemical analysis of representative slippery mutant RNAPs confirmed involvement of this region of the β subunit in regulation of transcription slippage.

## EXPERIMENTAL PROCEDURES

*Molecular Biology Reagents and Techniques*—Standard molecular biology and DNA techniques are as described (40). Reagents for PCR were from Invitrogen, NTPs were from GE HealthCare, and chemicals were from Sigma-Aldrich. DNA and RNA oligonucleotides were from IDT (San Diego, CA).

*Bacterial Strains and Bacterial Techniques*—Bacterial strains used in this study are *E. coli* K-12 strain MG1655 and its derivatives (Tables 1 and 2). The bacterial techniques and media used have been described (41). The β-gal activities (Miller units) were assayed by using overnight cultures grown in LB, as described (41). To correct for potential variations in different experiments, wild type controls were always included, and at least two duplicates for each of the strains tested were assayed in independent experiments. Random mutations in a plasmid-borne *rpoB* gene were introduced in an *E. coli* mutator strain XL1-Red (*XL1-Red*, from Stratagene) according to the manufacturer's manual.

*Strains and Plasmid Constructions*—Various mutations in *rpoB* were constructed using the Lambda Red-mediated recombineering method (42, 43). To make elongation slippage fusion strains, single-stranded oligonucleotides containing a

50-nt segment of *lacI* that encodes amino acid residues 16–33, a 9–10-nt spacer, and a 53-nt segment of *lacZ* that encodes amino acid residues 15–33 were used to replace the chromosomal *lacI-lacZ* region of the NC397 strain (44). Then the *lacI* promoter region of the resulting strains was replaced with the *tac* (or *tac**) promoter (pKK223-3; Pharmacia) using a 1-kb PCR fragment, in which a *cat* cassette (45) was flanked by the *mhpR* and *lacI* sequences using the following two primers: DJ24F, 5′-CTGAATCTGGTGTATATGGCGAGCGCAATGACCATTGAAACCTGTGACGGAAGATCACTTCGC-3′; and DJ24R, 5′-TGGTTTCACATTCACCACCCTGAATTGACTCTCTTCCGCCACACATTATACGAGCCGATGATTAATTGTCAACTAAGGGCACCAATAACTGCC-3′. The resulting constructs were confirmed by DNA sequencing. Those fusions were moved into MG1655 by P1 transduction, and the transductants were selected on LB plates containing chloramphenicol (15 $\mu$g/ml) and then screened for appropriate Lac phenotypes. Alternatively, similar fusions were constructed in derivatives of MG1655 harboring a plasmid-borne Lambda Red system that could be cured at ≥37 °C (46). New *rpoB* Rif$^r$ mutations were made by allele exchange with single-stranded oligonucleotides in strains that contained the *rpoC-his* tag fusion immediately linked to a *kan* cassette as verified by DNA sequencing. The resulting *rpoB* Rif$^r$ alleles were then introduced to different strains by phage P1 transduction. The transductants were selected on LB plates containing 30–50 $\mu$g/ml of kanamycin followed by screening of the Rif$^r$ phenotype.

The plasmid pDJ853, which contained the *rpoB-his* tag fusion, was constructed in two steps. First, a 0.9-kb SphI-SacI fragment in the wild type *rpoB* derivative of pXT7$\beta$ (47) was replaced with a ~110-bp SphI-SacI DNA fragment that encoded the last 24 amino acids of the $\beta$ subunit and the additional GGHHHHHH His tag residues to yield plasmid pDJ2080His (pT7wt *rpoB-his*). Second, a 1.6-kb HindIII fragment from pDJJ11 (48) that contained the *rplJL* promoter and the genes at its normal location before the *rpoB* gene was inserted into the HindIII site of pDJ2080His, resulting in pDJ853 (pRplJL-*rpoB-his*) or p*rpoB*.

*RNAP Purification and Transcription in Vitro—E. coli* RNAP carrying a $His_6$ tag at the C terminus of the $\beta'$ subunit (from wild type and six *rpoB* mutants) was immobilized on $Ni^{2+}$-NTA-agarose beads (Qiagen) directly from a crude cell lysate. The cells were grown in 8 ml of LB to an optical density at 600 nm of 0.8–1, centrifuged (Eppendorf 5804R, rotor A-4-44: 5,000 rpm, 6 min), and resuspended in 350 $\mu$l of lysis buffer (300 mM Tris acetate, pH 7.9, 100 mM potassium acetate, 10 mM $MgCl_2$, 1 mM EDTA, 4 mM 2-mercaptoethanol). All of the steps were performed at 4 °C. The cells were sonicated using a microprobe tip and Sonicator-Ultrasonic Processor VHX 750 watt (model GEX 750; PG Scientific) by five cycles of a 5-s pulse and 45-s cooling periods. The samples were centrifuged (10,000 rpm, 10 min). The supernatant (~300 $\mu$l) was transferred to a 1.5-ml Eppendorf tube and mixed with 100 $\mu$l of 30% suspension of $Ni^{2+}$-NTA-agarose beads, which was prewashed with transcription buffer as described previously (49), and the 200 $\mu$l of premixed 3 M KCl with 30 mM of imidazole (pH 7.9) was added. The samples were shaken for 30 min (1,100 rpm) and centrifuged on the table-top centrifuge, and the supernatant was discarded. The $Ni^{2+}$-NTA-agarose beads were washed with transcription buffer again, and the immobilized RNAP was used in transcription assays. The immobilized RNAP was ~80% pure with the yield ~1–2 $\mu$g/1 ml of the culture.

Ternary elongation complexes (TEC) were assembled with the following DNA and RNA oligonucleotides: RNA9, 5′-AUC GAG AGG-3′; RNA10, 5′-AUCGAGAGGG-3′; NDS79 (nontemplate DNA strands 79 nt long), 5′-CCT ATA GGA TAC TTA CAG CCA TCG AGA GGG ACA CGG CGA ATA GCC ATC CCA ATC CAC ACG TCC AAC GGG GCA AAC CGT A-3′; TDS76 (template DNA strand 76 nt long), 5′-GGT TTG CCC CGT TGG ACG TGT GGA TTG GGA TGG CTA TTC GCC GTG TCC CTC TCG ATG GCT GTA AGT ATC CTA TAG G-3′; NDS48, 5′-GGT ATA GGA TAC TTA CAG CCA TCG AGA GGG AAA AAA AAA CGA GGC GAA-3′; TDS48, 5′-TTC GCC TCG TTT TTT TTT CCC TCT CGA TGG CTG TAA GTA TCC TAT ACC-3′; NDS60, 5′-GGT ATA GGA TAC TTA CAG CCA TCG AGA GGG AAA AAA AAA CGA GGC GAA TAG AGA ACC CAA-3′; and TDS60, 5′-TTG GGT TCT CTA TTC GCC TCG TTT TTT TTT CCC TCT CGA TGG CTG TAA GTA TCC TAT ACC-3′. TDS62/NDS62 oligonucleotides were similar to TDS48/NDS48, except they were longer and contained 11-nt homopolymeric tracts.

Assembly of TEC9 (number indicates the RNA length in the TEC is 9 nt long, RNA9) on the beads, washing, elution, and 5′ RNA labeling were performed as described (50). For the bulk elongation assay (see Fig. 3), the 5′-labeled RNA9 and nonlabeled TDS76/NDS79 DNA oligonucleotides were used, and the reaction was performed in solution after elution of the TEC9 with imidazole. The RNA in TEC9 was elongated to 20-nt length with ATP, CTP, and GTP (10 $\mu$M each) for 1 min at room temperature. 10 $\mu$M UTP was added, at different times the reaction was stopped with gel loading buffer, and the products were subjected to PAGE as described (50). For the slippage assay measuring the rate of ATP incorporation by slippage (see Fig. 4), another TEC9 was made using nonlabeled RNA9 and TDS48/NDS48 oligonucleotides and elongated to TEC10 with 0.3 $\mu$M [$\alpha$-$^{32}$P]GTP (3000 Ci/mmol; PerkinElmer Life Sciences) for 4 min followed by washing with transcription buffer. The slippage reaction was performed on $Ni^{2+}$-NTA beads. To initiate slippage, ATP (10 $\mu$M) was added to TEC10 for different times, and the samples were processed as described above. The assay that was established to detect insertions and deletions during elongation on the 9A (or 11A) track (see Fig. 5) was similar to the slippage assay except that the longer TDS60 template and RNA10 primer were used, and a three times larger amount of the beads and the RNA-DNA oligonucleotides were employed. Also, labeling of the RNA with [$\alpha$-$^{32}$P]CTP was used to replace the labeling with [$\alpha$-$^{32}$P]GTP. TEC10 was directly assembled on TDS60/NDS60 (for 9A tract) or TDS62/NDS62 (for 11A tract) with unlabeled RNA10 followed by the addition of a mixture of the nonlabeled ATP (10 $\mu$M), CTP (100 $\mu$M), and 0.8 $\mu$M [$\alpha$-$^{32}$P]CTP (3000 Ci/mmol; PerkinElmer Life Sciences) in 150 mM KCl for 7 min (TEC10 → TEC20 or TEC22 reaction). The beads were washed with transcription buffer to remove the labeled NTPs, and the samples were processed for PAGE as described above.

## RESULTS AND DISCUSSION

*Rationale*—Identification of *E. coli* RNAP mutations affecting transcription slippage during elongation involved monitoring expression of a reporter gene (*lacZ*) carrying insertion of a homopolymeric A tract in the coding region of β-gal (27). For instance, the insertion of a 9-nt-long A tract and 1-nt deletion of the *lacZ* sequence adjacent to the tract generated a frameshift that inactivated the ORF encoding β-gal. The advantage of the *E. coli lacZ* reporter was that the change in color of colonies on indicator McConkey lactose (MacLac) plates could directly identify potential mutations in RNAP that alter transcription slippage under the conditions used. Altered expression of the *lacZ* reporter in the RNAP mutants could be due to nonslippage effects, such as changes in transcription initiation compared with wild type. To identify and discard those RNAP mutants in which the color phenotype derived from an effect on the promoter activity of the reporter gene, we introduced an additional *lacZ* reporter carrying a nonslippery in-frame 9-nt-long spacer insertion to normalize slippage activity to promoter strength. To further validate this approach, we performed biochemical analysis of the mutant RNAPs *in vitro* for their elongation properties and slippage at the homopolymeric A tracts.

*Construction of in Vivo Slippage Reporter Strains*—To avoid complications caused by plasmid copy number variations, we engineered a chromosomal-based slippage strain rather than a plasmid-borne system as previously described (27). The genome region encompassing the coding sequences for the C terminus of LacI and the promoter and N terminus of LacZ were deleted, and the two genes were joined with a spacer resulting in a *lacI′*-spacer-*′lacZ* fusion (Fig. 1*A*). The spacer AAAAAAAAA(−1), called 9A(−1), contained an insertion of a homopolymeric run of 9A, with the number in the parentheses indicating a nucleotide deletion in reading frame relative to the downstream fused *′lacZ* gene. A 0 frame is defined as the same reading frame as *′lacZ*; a −1 is out of frame by a one nucleotide deletion (27). Thus, for restoration of *lacZ* ORF from the 9A(−1) strain, a 1-nt insertion or a 2-nt deletion would be needed during transcription through the 9A track. We also made two nonslippage strains, one with spacer sequences of AAAATAAAA(−1) called 4AT4A(−1) as an out of frame control and another of AAAAATAAAA(0) called 5AT4A(0) as an in-frame control. These spacer variants were important for the analysis of slippage phenotypes of wild type and mutant RNAPs (see below). Hereafter these strains are named after their spacer designations.

To develop a genetic scheme for the isolation of RNAP mutants that alter transcription slippage during elongation, it was critical to adjust expression of the reporter to the level enabling identification of the candidate mutant colonies by their color on indicator MacLac plates. Our initial studies found that although the *lacI* promoter was too weak, the *tac* promoter was too strong (data not shown) to be used for the identification of RNAP mutants. To tune the expression levels of the *lacI′*-spacer-*′lacZ* fusions, the chromosomal *lacI* promoter in each of these strains was replaced with a mutated *tac* promoter (p*tac**) carrying a change of A for C in the "−35" region (TTGAC***C***) compared with the (TTGAC***A***) *tac* promoter. The p*tac** promoter supported a level of the β-gal expression suitable for identification of slippage mutations on MacLac plates. For example, the expression level of the *lacZ* fusion in the 9A(−1) slippage strain was such that single colonies of the cells appeared white after ~15 h of incubation, turning to pink/red after ≥24 h of incubation on MacLac plates at 37 °C. The color of colonies was also affected by temperature during incubation. This phenotype provided a useful screening scheme for the isolation of potential RNAP mutants by looking for color changes of colonies on the MacLac plates under the same growth conditions (Fig. 1*B*).

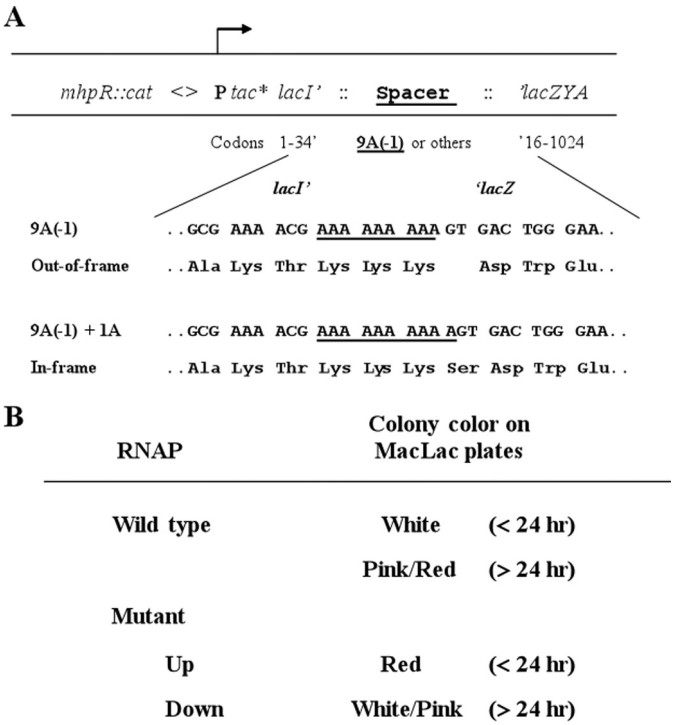


**B**

| RNAP | Colony color on MacLac plates | |
|---|---|---|
| Wild type | White | (< 24 hr) |
| | Pink/Red | (> 24 hr) |
| Mutant | | |
| Up | Red | (< 24 hr) |
| Down | White/Pink | (> 24 hr) |

FIGURE 1. *A*, schematic illustration of a set of chromosomal constructs used for the isolation and characterization of RNAP slippage mutants. These reporter strains differed in the spacer sequence and the resulting reading frame relative to the fused *′lacZ* gene. The numbers of residues of the N-terminal of LacI′ 1–34 and C-terminal of ′LacZ, respectively, are indicated. As examples, the flanking DNA sequences of *lacI′* and *′lacZ* (and their codons) that are fused with the 9A(−1) spacer are shown; amino acid residues, which are encoded by the spacer sequences (*underlined*), either out-of-frame or restored in-frame with the *lacZ* because of slippage, are indicated. The *tac** promoter had a −35 mutation (TTGAC***A*** → TTGAC***C***) compared with the wild type *tac* promoter. Selection for the *cat* cassette facilitated the introduction of the constructs into different strain backgrounds. See text for details. *B*, identification of potential RNAP slippage mutants using the 9A(−1) reporter. For wild type RNAP, the expression of the out of frame *′lacZ* was low, and colonies were a white color on MacLac plates after an overnight incubation (<24 h) and became a pink/red color after a prolonged incubation (>24 h). RNAP mutants with increased expression of the reporter (Up) exhibited red colonies on MacLac plates after less than 24 h of incubation. However, RNAP mutants with decreased expression of the reporter (Down) formed white/pink colonies even after a prolonged incubation.

The β-gal activity of the slippage strain and nonslippage control strains were determined (Table 3). The activity produced from the in-frame nonslippage 5AT4A(0) strain was ~655 units, whereas the out-of-frame nonslippage 4AT4A(−1) reporter produced ≤1 unit of β-gal. Importantly, the 9A(−1) slippage reporter produced ~35 units of β-gal, indicating that wild type RNAP was undergoing slippage at homopolymeric A/T runs *in vivo*, as was shown for runs of 11A nt (27). The

**TABLE 3**
**β-Gal activities of different reporter strains**

| Reporter stain[a] | β-Gal activities |
|---|---|
| 9A(−1) | 35 ± 4 |
| 4AT4A(−1) | ~1 |
| 5AT4A(0) | 655 ± 33 |

[a] The spacer sequence and the reading frame relative to the fused *'lacZ* in parentheses are described in the text.

colonies of the 9A(−1) reporter strain were white to pink/red on MacLac plates, depending on the incubation time and temperature as described above.

*Isolation of Plasmid-borne rpoB Mutations Causing an Increased Elongation Slippage Phenotype*—The *rpoB* gene encodes the β subunit, which forms a part of the active center in RNAP. The β subunit also encases the RNA side of the RNA-DNA hybrid in the elongation complex (1, 2). Moreover, certain *rpoB* mutations affect slippage during initiation (38).[7] Reasoning that some RNAP mutations conferring an enhanced slippage phenotype during elongation could be lethal, we decided to isolate *rpoB* mutations initially from a plasmid-borne gene by looking for increased *lacZ* expression in the presence of a chromosomal wild type *rpoB* gene in the 9A(−1) reporter strain.

A new *rpoB* expression construct with specific features was needed for the isolation of *rpoB* mutants. We constructed a plasmid-borne *rpoB* gene (pDJ853) p*rpoB* with the following properties: (i) the expression of the *rpoB* gene is constitutive at a level that was able to complement chromosomal *rpoB* temperature-sensitive mutants (51) without affecting the growth of wild type cells (data not shown); and (ii) the *rpoB* gene on the plasmid is fused to a hexahistidine tag at the C terminus of β, so that RNAP carrying the mutation can be separated from the wild type counterpart for *in vitro* analysis of slippage. When the p*rpoB* plasmid was introduced into the 9A(−1) reporter strain, colonies appeared white on a MacLac+Amp plate after overnight incubation at 37 °C, similar to the strain without the plasmid.

To introduce random mutations in *rpoB*, the p*rpoB* plasmid was propagated in an *E. coli* mutator strain (*XL1-Red*; Stratagene). The mutagenized p*rpoB* pools were introduced into the 9A(−1) reporter strain by transformation. The transformants were screened on the MacLac+Amp indicator plates at different temperatures. Occasionally, fish eye (red in the center of a white colony) or red colonies appeared, indicative of increased expression of the 9A(−1) *lacZ* fusion. These cells exhibiting a "$Lac^+$" phenotype harbored p*rpoB* candidates for RNAP slippage mutants. Plasmid DNA from each of the candidates was purified and reintroduced into a Δ*recA* derivative of the 9A(−1) reporter strain to prevent recombination between the chromosomal wild type *rpoB* gene and a plasmid-borne *rpoB* mutation. All of the six p*rpoB* mutations that exhibited a $Lac^+$ phenotype after retransformation were sequenced, and changes in the β subunit are shown in Table 4. All of these mutations conferred a slow growth phenotype on the host cells at 30 °C, and cells harboring the plasmid-borne M1273I mutation had an additional temperature-sensitive phenotype at 42 °C.

[7] D. J. Jin, unpublished results.

**TABLE 4**
**Effects of plasmid-borne rpoB mutations on elongation slippage in vivo**

The values are the averages of at least two independent experiments. Each experiment was performed with minimum of two repetitions. The values of different independent experiments generally deviated less than 10% from the average value. WT indicates 35 ± 4 units of β-Gal in 9A(−1) and 655 ± 33 units in 5AT4A (see Table 3).

| RNAP mutation | | Relative β-Gal activity | | Relative slippage phenotype (9A(−1)/5AT4A(0)) |
|---|---|---|---|---|
| Amino acid change | Codon change | In 9A(−1) | In 5AT4A(0) | |
| Wild type | | 1.0 | 1.0 | 1.0 |
| D444G | GAT → GGT | 1.7 | 1.0 | 1.7 |
| R451C | CGT → TGT | 1.8 | 1.1 | 1.6 |
| A543V | GCA → GTA | 1.3 | 1.1 | 1.2 |
| G570D | GGT → AGT | 1.6 | 1.3 | 1.2 |
| R687C | CGT → TGT | 1.8 | 1.1 | 1.6 |
| M1273I | ATG → ATA | 1.9 | 1.3 | 1.5 |

The β-gal expression level of the *lacZ* fusion in the Δ*recA* 9A(−1) reporter strain harboring each p*rpoB* mutation, as well as the wild type p*rpoB* clone, was determined (Table 4). Relative β-gal activity of each mutant was calculated by dividing the β-gal activity from cells with an *rpoB* mutation over that of the cells containing the wild type plasmid. Consistent with the $Lac^+$ phenotypes on MacLac+Amp indicator plates, all of the six plasmid-borne p*rpoB* mutations increased expression of the 9A(−1) out-of-frame *lacZ* fusion compared with wild type (Table 4). To correct for potential effects of the mutations on transcription initiation at the p*tac** promoter, the plasmids with the six *rpoB* mutations and wild type were introduced into a Δ*recA* derivative of the 5AT4A(0) nonslippage control strain, and the relative β-gal activity of the 5AT4A(0) cells harboring each of these mutations was calculated similarly (Table 4). A relative slippage phenotype of each RNAP mutant was estimated as a ratio of the two relative β-gal activities (Table 4). By this analysis, four of the six mutants increased elongation slippage ≥1.5-fold compared with wild type.

*Isolation of Chromosomal rpoB $Rif^R$ Mutants with Altered Elongation Slippage Phenotypes*—We noted that all of the six plasmid-borne p*rpoB* slippage mutations, with the exception of M1273I, are located in the elongation complex bordering the RNA strand of the 9-bp RNA-DNA hybrid region (Fig. 2); in particular, two of them (G570D and R687C) affected amino acid residues harboring other previously identified mutations that cause resistance to the antibiotic rifampicin ($Rif^R$) (48, 52). Although none of our new slippage mutants conferred a $Rif^R$ phenotype, this observation prompted us to test the effects of known chromosomal *rpoB* $Rif^R$ mutations on elongation slippage.

*E. coli* $Rif^R$ mutations are exclusively located in the *rpoB* gene and affect 25 clustered amino acid residues of the fork domain of the β subunit (48, 52, 53). All are clustered along the RNA flank of the 9-bp RNA-DNA hybrid region near the active center of RNAP (Fig. 2; see also Fig. 6*B*, colored in yellow). In addition to testing all chromosomal $Rif^R$ mutants from our collection (48), we also generated many other chromosomal *rpoB* $Rif^R$ mutations (52) by Lambda Red recombineering (43, 54). All of these $Rif^R$ mutations were made in the strain carrying the His-tagged *rpoC* gene on the chromosome. We examined more than 50 $Rif^R$ mutations affecting 24 positions (Tables 2) for their

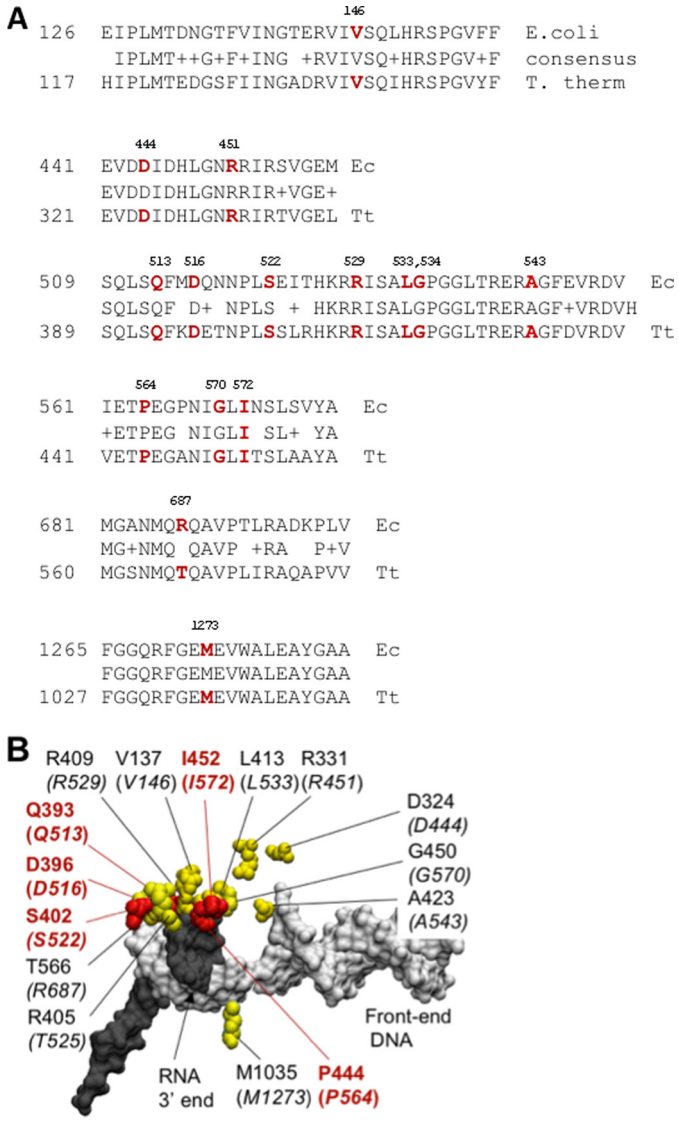


FIGURE 2. **Slippage mutations in the β subunit have close proximity to the 9-bp RNA-DNA hybrid.** *A*, a sequence alignment of the Rif-binding region in the β subunit of *T. thermophilus* (*Tt*) and *E. coli* (*Ec*) RNAP (the fork domain). The amino acid residues harboring both the plasmid-borne and the chromosomal *rpoB* mutations that affect slippage on a 9A tract *in vivo* are shown in *red*. *B*, the amino acid residues of the β subunit involved in control of slippage are highly clustered (shown in *yellow*) in the structure of the *T. thermophilus* RNAP TEC (Protein Data Bank code 2O5J) (2). The corresponding positions in *E. coli* RNAP are shown in *brackets*. The residues carrying mutations with the confirmed slippage phenotype *in vitro* are highlighted in *red*. The RNA transcript and the template DNA are colored *gray* and *white*, respectively.

effects on elongation slippage in the 9A(−1) reporter strain. Many of the Rif$^R$ mutants had a Lac$^+$ phenotype on MacLac plates. Interestingly, we also identified several Rif$^R$ mutants with a reduced Lac colony phenotype because they formed white colonies after prolonged incubations (>24 h) compared with wild type under the same conditions.

Next, we determined the relative β-gal activities of the affected mutants in both the 9A(−1) and 5AT4A(0) reporter strains (Table 5). As described above, a relative slippage phenotype of a RNAP mutant was estimated as a ratio of the two relative β-gal activities. This analysis yielded 14 *rpoB* Rif$^R$ mutants affecting 10 positions in the β subunit that altered elongation slippage compared with wild type. Among them, 11

**TABLE 5**

**Effects of the chromosomal rpoB Rif$^R$ mutations on elongation slippage in vivo**

The values are the averages of at least two independent experiments. Each experiment was performed with minimum of two repetitions. The values of different independent experiments generally deviated less than 10% from the average value.

| *rpoB* mutation | Relative β-Gal activity in | | Relative slippage phenotype (9A(−1)/5AT4A(0)) |
|---|---|---|---|
| | 9A(−1) | 5AT4A(0) | |
| Wild type | 1.0 | 1.0 | 1.0 |
| V146F | 2.1 | 1.3 | 1.6 |
| V146G | 2.2 | 1.4 | 1.6 |
| Q513P | 3.0 | 0.9 | 3.3 |
| D516N | 0.6 | 1.2 | 0.5 |
| S522F | 1.8 | 1.1 | 1.6 |
| S522Y | 2.5 | 1.0 | 2.5 |
| T525R | 2.4 | 1.0 | 2.4 |
| R529H | 1.9 | 1.2 | 1.6 |
| Δ532 | 2.3 | 1.4 | 1.6 |
| P564L | 3.1 | 1.5 | 2.0 |
| G570C | 4.1 | 2.4 | 1.7 |
| G570Q | 2.5 | 1.3 | 1.9 |
| I572T | 0.8 | 1.2 | 0.7 |
| I572N | 0.8 | 1.2 | 0.7 |

Rif$^R$ mutants increased elongation slippage, and three had decreased slippage. The positions of these mutations at the RNA-DNA hybrid region of RNAP are shown (Fig. 2), and the results strongly indicate that amino acid residues in this region are important for slippage.

*Analysis of the Mutant RNAPs in Vitro*—To confirm the slippage phenotypes of the *rpoB* mutants, we performed biochemical analysis of representative mutant RNAPs. We chose six chromosomal Rif$^R$ mutants affecting five amino acid positions because they had the strongest slippage phenotypes *in vivo*. The *rpoB* mutants Q513P, S522Y, and P564L were "up" mutants, and D516N, I572N, and I572T, were "down" mutants. These strains, as indicated above, also carried a functional hexahistidine-tagged β′ subunit, which allowed the rapid pulldown and purification of RNAP from the crude lysate by immobilization on $Ni^{2+}$-NTA-agarose beads (49, 55). Each of the purified enzymes was assembled into a TEC with a synthetic RNA-DNA scaffold, and the bulk elongation rate for each mutant RNAP was tested in a single-round "runoff" assay with 10 μM NTP (Fig. 3). The Q513P, D516N, P564L, and I572T mutants had an elongation rate similar to the wild type enzyme. The I572N were ~2-fold slower, and S522Y was ~2-fold faster than the wild type enzyme in a single round transcription. Because of the relative minor effect on the elongation rate in these bulk elongation assays, we concluded that these mutations do not cause a significant change in the regular catalytic activity of RNAP.

Next, we evaluated slippage pattern by the mutants on a RNA-DNA scaffold containing a tract of 9As in the transcript to match the 9A spacer sequence used for the *in vivo* screening. Slippage during unimpeded transcription of 9A tract generates both insertions and deletions, and their ratio should depend on RNAP dwell time at adenine positions within the 9A tract. For instance, a prolonged pausing at the +8 position of the tract should equally promote deletions and insertions by forward and backward shift of the RNA strand relative to the DNA, respectively. In contrast, the dwelling at the last 9 position should increase insertions only, because deletions are not allowed at the end of the tract. To produce deletions, RNAP should shift forward on DNA together with the nascent RNA,

whereas insertions result from a shift in the opposite direction. Thus, RNAP halted at the end of the tract is unable to shift further forward without producing a mismatch between the 3′ end of the RNA and the DNA.

To separate slippage in the tract from that at the end of the tract, we developed two *in vitro* assays. The first assay aimed to determine slippage leading to insertions, and it included a prolonged halting RNAP at the end of 9A tract in the absence of all NTPs except ATP (Fig. 4). For this purpose, different TEC9 was assembled with the 9-nt RNA primer (5′-AUCGAGAGG) hybridized 1 base pair upstream from the coding region for the 9A tract. The RNA in the TEC9 was extended 1-nt by adding [$\alpha$-$^{32}$P]GTP to form TEC10 labeled at its 3′ end before the 9A tract. By adding ATP, the TEC10 transcribed the entire 9A tract followed by pausing at the last adenine in the tract because of the lack of the next CTP. A substantial fraction of RNAP was arrested at the last adenine of the 9A tract, which is consistent with previous findings that A/T-rich sequences cause arrest of RNAP (56, 57). In the absence of slippage, TECs halted at the end of the 9A tract generate a 19-nt RNA transcript (TEC19). In the experiment of Fig. 4, continuous slippage at the last base of 9A tract produced a distribution of slippage products longer than 19 nucleotides, which were processively elongated by slippage. The slippage rate was determined as the average number of AMP molecules added to the RNA per second (Fig. 4*A*). Relative to wild type, the D516N, P564L, and I572T mutants showed an increase of the slippage rate; the Q513P mutant showed a slower slippage rate, and S522Y and I572N mutants were similar to the wild type enzyme (Fig. 4, *left panel*). Importantly, the slippage at the 9A tract by the assembled TEC showed the same rate of AMP incorporation as that observed during transcription of the same tract initiated from a promoter (T7A1 promoter; data not shown). This result justified our employment of RNA-DNA scaffolds for testing slippage. Transcription slippage requires uninterrupted 9A track (Table 3). Accordingly, an interruption of 9A tract at the fifth position

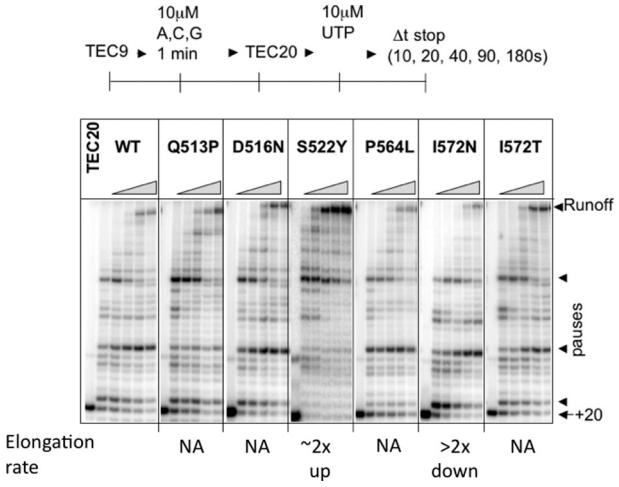


FIGURE 3. **General *in vitro* elongation properties of the *rpoB* mutants.** A single round of transcription was performed with 10 $\mu$M NTPs and 5′-labeled RNA9 primer in two steps as indicated in the scheme at the *top*. TEC20 once formed was elongated with four NTPs for 10–180 s to form a runoff RNA. The *arrow* marks the position of the 20-nt RNA in TEC20; the *arrowheads* mark the 45-nt runoff RNA and the major transcription pause sites. The *numbers* at the *bottom* indicate the effects of a mutation (fold increase or decrease) on the bulk elongation rate, and *NA* indicates that the rate was not affected relative to wild type under the low NTP conditions. The similar results were obtained with high 200 $\mu$M NTPs (data not shown).

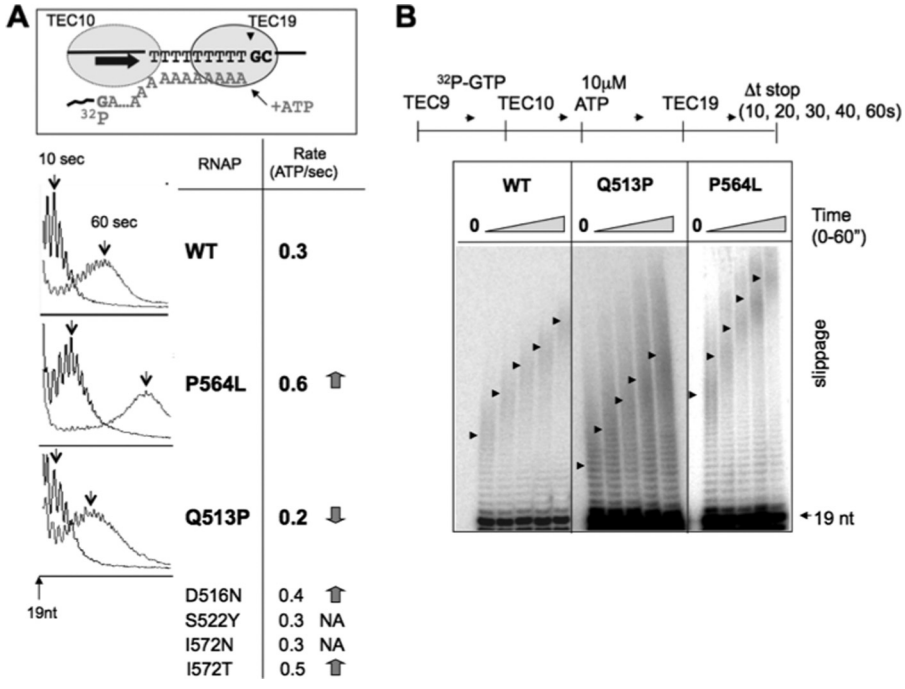


FIGURE 4. **Processive slippage of RNAP halted at the end of the 9A tract.** *A*, a cartoon at the *top* depicts TEC19 labeled at the +10G position of the RNA that idles at the end of the 9A tract in the presence of 10 $\mu$M ATP. The graphs show the extension of the slippage products beyond the 19-nt length by slippage after 10 s (*arrows*) and 60 s (*arrows*) of incubation with ATP (WT and $\beta$-P564L and $\beta$-Q513P mutants). The *second column* presents an average slippage rate for six mutants calculated as a number of ATP molecules added to the RNA/s. The decrease or increase of the ATP addition rate relative to WT is indicated by *downward* and *upward arrows*, respectively, and where *NA* means not affected. *B*, the representative autoradiogram shows time-dependent slippage in TEC19 formed by $\beta$-Q513D, Q513P, and P564L mutants. The *arrows* indicate the center of the peak for the distribution of the slippage products at each time point after ATP addition.

with a single U or G residue and replacement of the 9A track with 9C tract completely inhibited slippage *in vitro* (data not shown). Thus, the processive AMP addition in the assay of Fig. 4 was due to slippage as opposed to the multiple AMP misincorporations.

Although providing important information on the chemical rate of slippage, the assay of Fig. 4 did not allow direct comparison of the *in vitro* slippage with the *in vivo* data obtained with the 9A(−1) reporter strain. Slippage *in vivo* produces either insertions or deletions, whereas the assay of Fig. 4 was designed to detect insertions only. In addition, transcription through the 9A tract *in vivo* occurs without stopping RNAP at the end of the tract by CTP deprivation. To better match these *in vivo* conditions and to evaluate how the *rpoB* mutations affect deletions in the tract, we modified the assay of Fig. 4 by simultaneous addition of ATP and $\alpha$-$^{32}$P-labeled CTP that should generate a transcription complex with a 20-nt RNA if no slippage occurred (TEC20; Fig. 5). We assembled nonlabeled TEC10 with the 3′ end of its RNA located immediately upstream from the first residue of 9A tract (5′-AUCGAGAGGG) on template. By adding ATP and labeled CTP, the TEC10 proceeds to the end of the 9A tract by incorporation of nonlabeled AMP, incorporates a single labeled CMP beyond the A tract, and then stalls because of the lack of the next complementary base, GTP (Fig. 5). The modified assay served two purposes: (i) it limited any slippage to a short time period before incorporation of the [$^{32}$P]CMP occurred, and (ii) it produced the 3′ end-labeled RNA containing the A tract followed by the cytosine. The 3′-labeled RNA products could easily be examined for slippage by urea-PAGE as described and summarized in the *table panel* of Fig. 5.

The result of Fig. 5 demonstrated that the majority of the *rpoB* mutants had the altered slippage pattern. Q513P mutant showed dramatic increase in deletion of 1 adenine (1A) from the 9A tract and almost complete elimination of 1A insertion. In contrast, P564L mutant significantly increased 1A insertion and decreased 1A deletion. Strikingly, the two mutants exhibited the opposite slippage directionality. D516N, I572N, and I572T mutants produced less 1A insertion than the wild type without affecting 1A deletions. Finally, S522Y mutant showed no difference in slippage from the wild type.

A bias toward insertions or deletions during slippage may depend on how rapidly RNAP transcribes through the 9A tract. As described above, the complex that has reached the end of the tract retains the ability to generate insertions but not deletions. Therefore, RNAP mutants that pause more than the wild type before the end of the 9A tract may make more deletions, whereas the mutants that induce more pausing at the end of the 9A tract may make more insertions.

Most of these results were consistent with the *in vivo* data. For example, the up slippage phenotypes of P564L mutant could be explained by its enhanced frequency for 1A insertion in the 9A(−1) *lacZ* reporter *in vivo*, which was designed to look primarily for 1A insertions to the 9A tract for restoration of the LacZ open reading frame (Fig. 1). Conversely, the down slippage phenotypes of D516N, I572N, and I572T could be explained by their reduced frequency for 1A insertion compared with wild type. The Q513P mutant showed the most dramatic change in slippage pattern compared with the wild type

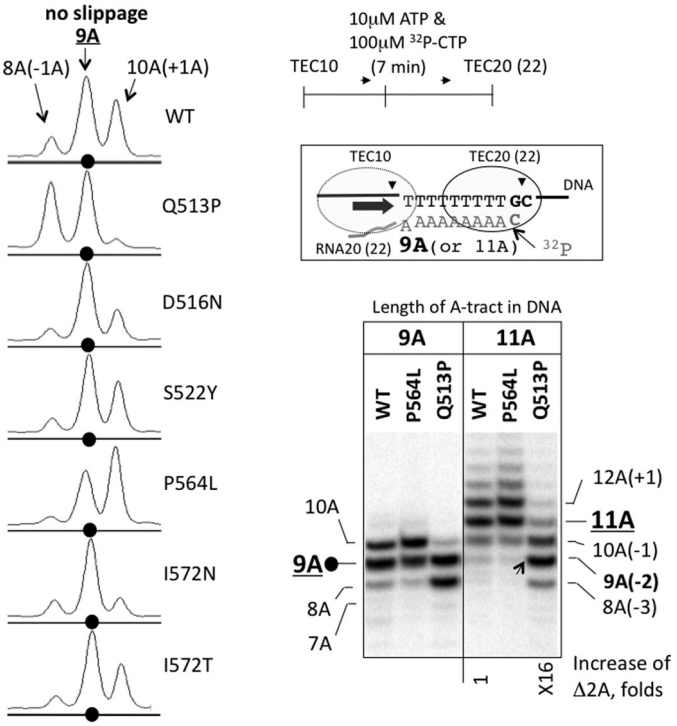


| Rif-r rpoB mutation | Deletion -1A | Insertions +1A | Ins/Del ratio | Elong. rate | Slippage *in vivo*, 9A(-1) |
|---|---|---|---|---|---|
| **WT** | **0.1** | **0.3** | **3** | **-** | **1** |
| Q513P | 0.4 | < 0.1 | < 0.25 | NA | 3.3 |
| D516N | 0.1 | 0.2 | 2 | NA | 0.5 |
| S522Y | 0.1 | 0.3 | 3 | ↑ | 2.5 |
| P564L | < 0.1 | 0.6 | > 6 | NA | 2.0 |
| I572N | 0.1 | 0.2 | 2 | ↓ | 0.7 |
| I572T | 0.1 | <0.3 | 3 | NA | 0.7 |

FIGURE 5. **Detection of deletions and insertions in the RNA during transcription through 9A and 11A tracts *in vitro*.** The cartoon shows the 3′-labeled TEC20 (or TEC22) halted one nucleotide downstream from the end of the 9A (or 11A) tract after elongation of unlabeled TEC10 with ATP and [$\alpha$-$^{32}$P]CTP. The autoradiogram depicts the slippage products (7A, 8A, and 10A RNAs for 9A tract; 8–10A and >11A RNAs for 11A tract) generated by the WT RNAP and $\beta$-P564L and $\beta$-Q513P mutants relative to the expected 9A or 11A transcript. The *number* under the autoradiogram shows the increase in the yield of 2A deletion in 11A tract caused by $\beta$-Q513P mutation. The phosphorimaging scans (on the *left*) reveal the difference in the pattern of slippage products by the WT RNAP and the six *rpoB* mutants. *Black dots* indicate the RNA product containing the 9A tract, and the slippage products are labeled according to the number of adenine residues in the tract. The *table panel* at the *bottom* summarizes slippage properties of the *rpoB* mutants. The *numbers* in the *second* and *third columns* represent the fraction of 1A deletion and 1A insertion normalized to the total amount of the CMP-labeled RNAs (include 8A, 9A, and 10A products). The *fourth column* shows the ratio between insertions and deletions for each mutant. The *fifth column* presents the effect of the mutations on elongation rate of RNAP on heteropolymeric DNA reproduced from the results of Fig. 3. The *last column* displays the relative slippage phenotype with the 9A(−1) reporter *in vivo* (from Table 4).

and all other *rpoB* mutants. Its up slippage phenotype *in vivo* could be explained by its strong bias toward making deletions, which would restore in-frame *lacZ* in the 9A(−1) reporter by the 2A deletion instead of 1A insertion. Although Q513P showed a sign of the increased 2A deletions *in vitro*, the sensitivity of our assay was not sufficient for reliable detection of multiple deletions in 9A tract. Therefore, we employed the longer 11A tract to test whether Q513P is capable for multiple deletions. The result of this assay was striking. The Q513P mutant showed a major ~16-fold increase of 2A deletion in

11A tract. The minor 3A deletion was also clearly detected with the mutant (Fig. 5). The decreased 1A insertion by Q513P mutant explained its decreased rate of processive AMP addition in TEC halted at the end of 9A tract by CTP deprivation (Fig. 4). On the other hand, this mutation had no apparent effect on NTP incorporation during bulk elongation under the condition used (Fig. 3). The Q513P mutant enzyme was reported to have an increased $K_m$ for purine nucleotides during elongation (58). We suggest that this mutation primarily affected slippage as opposed to the regular elongation pathway.

Other Rif$^R$ mutants, including T525R, R529H, G570C, and G570Q, did not show any effect on slippage in this *in vitro* assay (data not shown). The V146F and V146G mutations dramatically reduced the bulk elongation rate of RNAP during transcription of the 9A tract, which prevented us from determining the slippage pattern for these mutants.

*Summary of Slippage Effects*—The slippage mutants analyzed in this work fell into four categories: (i) mutations that increase slippage efficiency (the combined yield of insertions and deletions) and additionally increased the intrinsic tendency of the wild type enzyme to make more insertions than deletions (defined here as slippage directionality) (P564L); (ii) mutations that change slippage directionality but not slippage efficiency (Q513P); (iii) mutations that decreased slippage efficiency; most of these mutations also affect slippage directionality by inhibiting insertions more than deletions (D516N, I572N, and I572T); and (iv) mutations that affect slippage *in vivo* but not *in vitro* (the chromosomal mutants: β-S522Y, T525R, R529H, G570C, and G570Q; and the plasmid-borne mutants: β-D444G, R451C, A543V, G570D, and R687C) (data not shown). The plasmid-borne β-M1273I mutant exhibited an extremely slow elongation rate *in vitro*, causing its complete arrest within the 9A tract, which did not allow its further analysis. The difference between the *in vitro* and *in vivo* results on several mutants could be attributed to the design of the *in vitro* assay involving a nonphysiologically low ATP concentration (cellular ATP concentration in the millimolar range rather than 10 μM used *in vitro*).

Fig. 6 shows the location of the mutated amino acid residues in the crystal structure of the *Thermus thermophilus* RNAP (TEC) (2). The majority of the mutations identified in our work affect residues encapsulating the 9-bp RNA-DNA hybrid at the bottom of the catalytic cleft in RNAP. In particular, β-Gln-513, Asp-516, Pro-564, and Ile-572 are sufficiently close to the 9-bp RNA-DNA hybrid to form hydrogen bonds with the RNA strand at nucleotide positions 3 and 4 upstream from the 3′ end of the transcript. The Rif-binding pocket in the β subunit is part of the fork region (residues 500–690), which undergoes a major conformational change during the switch of RNAP from initiation to elongation mode (2, 59). The fork region is an interface between the β and β′ subunits; the conformational change during TEC formation is proposed to promote closure of the β′ protein clamp with the β subunit around the RNA-DNA hybrid (2). After testing mutations within the 25 amino acid residues forming an extended binding pocket for rifampicin, we identified a small protein path forming an interface between the RNA strand of the hybrid and the fork domain of the β subunit involved in slippage both *in vivo* and *in vitro*. We suggest that

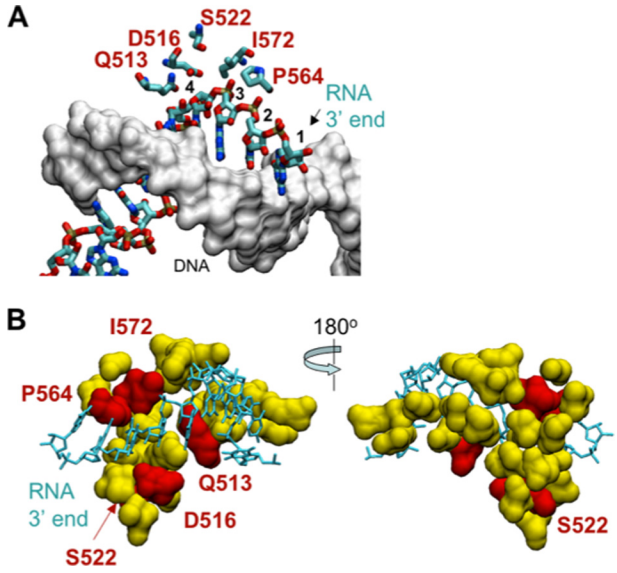


FIGURE 6. **A small segment of the fork domain in the β subunit is important for controlling transcription slippage.** *A*, a nucleic acid scaffold in the *T. thermophilus* RNAP TEC (Protein Data Bank code 2O5J) (2) and location of the slippage domain. The RNA strand in the 9-bp RNA-DNA hybrid is shown as a wire frame model, and the DNA strand is shown as a surface model (*gray*). The *arrow* indicates the 3′ end of the RNA, and individual residues in the 3′-proximal part of the RNA are *numbered* starting from the 3′ end. Amino acid residues contacting the RNA are shown. *B*, amino acid residues in the β subunit involved in formation of the Rif-binding pocket (25 residues of the fork domain are shown in *yellow*). *Red* highlights five amino acid residues that when mutated affect slippage both *in vivo* and *in vitro*. The RNA strand in the hybrid is shown as a wire frame model (*cyan*), and the DNA strand in the hybrid is omitted.

mutations in this region weaken the DNA clamp in the elongation complex, which facilitates spontaneous melting of the RNA-DNA hybrid leading to slippage. The present work analyzed the effect on slippage of mutations in a small region of the β subunit adjacent to the RNA-DNA hybrid. The approach used in this study will be useful to further identify other positions (non-Rif$^R$ sites) in the same region, as well as other regions in the β and β′ subunits that are important for transcription slippage.

A significant fraction of the mutations identified for increased slippage *in vivo* did not show effects on slippage *in vitro*. These mutations were primarily localized to the area of the protein around the DNA duplex downstream of the RNA-DNA hybrid in the elongation complex. Although several mutations from this class were localized near the RNA-DNA hybrid, the majority of them were not directly involved in interactions with the RNA strand in the hybrid. This class of mutations is likely to affect the interaction of RNAP with the front end DNA duplex in the elongation complex. They also may affect interaction of RNAP with transacting factors, which were not present in our "minimal" *in vitro* system. Alternatively, an increased slippage phenotype exhibited by these mutants *in vivo* may require a different concentration of ATP substrates or some other cellular conditions, which we cannot fully recapitulate *in vitro*. Transcription elongation in bacteria is coupled to translation. Therefore, some of the RNAP mutations might affect slippage indirectly by promoting translational frameshifts at the 9A tract in the *lacZ* mRNA (60). This group of mutants deserves further investigation.

*Summary Remarks*—We have developed a simple genetic system to isolate RNAP mutants that alter transcription slippage during elongation, complementary to an accompanying paper on slippage in yeast (39). We have identified the fork region in RNAP near the RNA-DNA hybrid as being important for slippage. Our successful isolation of the highly clustered fork mutants that decrease or increase slippage indicated that wild type bacterial RNAP is evolved for some slippage, which may be regulated according to the cellular conditions. Identification of several mutations that change slippage directionality argues that elongation intermediates leading to deletions and insertions include distinct conformations of RNAP. This work provides a basis for further elucidation of the elongation slippage mechanism responsible for out of DNA register errors in transcription.

*Acknowledgments—We acknowledge the highly interactive environment at the Gene Regulation and Chromosome Biology Laboratory and Zachary Burton for critical reading of the manuscript.*

## REFERENCES


1. Vassylyev, D. G., Vassylyeva, M. N., Zhang, J., Palangat, M., Artsimovitch, I., and Landick, R. (2007) Structural basis for substrate loading in bacterial RNA polymerase. *Nature* **448,** 163–168
2. Vassylyev, D. G., Vassylyeva, M. N., Perederina, A., Tahirov, T. H., and Artsimovitch, I. (2007) Structural basis for transcription elongation by bacterial RNA polymerase. *Nature* **448,** 157–162
3. Trinh, V., Langelier, M. F., Archambault, J., and Coulombe, B. (2006) Structural perspective on mutations affecting the function of multisubunit RNA polymerases. *Microbiol. Mol. Biol. Rev.* **70,** 12–36
4. Ebright, R. H. (2000) RNA polymerase. Structural similarities between bacterial RNA polymerase and eukaryotic RNA polymerase II. *J. Mol. Biol.* **304,** 687–698
5. Springgate, C. F., and Loeb, L. A. (1975) On the fidelity of transcription by *Escherichia coli* ribonucleic acid polymerase. *J. Mol. Biol.* **97,** 577–591
6. Strathern, J. N., Jin, D. J., Court, D. L., and Kashlev, M. (2012) Isolation and characterization of transcription fidelity mutants. *Biochim. Biophys. Acta* **1819,** 694–699
7. Shaw, R. J., Bonawitz, N. D., and Reines, D. (2002) Use of an *in vivo* reporter assay to test for transcriptional and translational fidelity in yeast. *J. Biol. Chem.* **277,** 24420–24426
8. Reynolds, N. M., Lazazzera, B. A., and Ibba, M. (2010) Cellular mechanisms that control mistranslation. *Nat. Rev. Microbiol.* **8,** 849–856
9. Libby, R. T., and Gallant, J. A. (1991) The role of RNA polymerase in transcriptional fidelity. *Mol. Microbiol.* **5,** 999–1004
10. Libby, R. T., Nelson, J. L., Calvo, J. M., and Gallant, J. A. (1989) Transcriptional proofreading in *Escherichia coli*. *EMBO J.* **8,** 3153–3158
11. Foster, P. L. (2007) Stress-induced mutagenesis in bacteria. *Crit. Rev. Biochem. Mol. Biol.* **42,** 373–397
12. Kireeva, M. L., Nedialkov, Y. A., Cremona, G. H., Purtov, Y. A., Lubkowska, L., Malagon, F., Burton, Z. F., Strathern, J. N., and Kashlev, M. (2008) Transient reversal of RNA polymerase II active site closing controls fidelity of transcription elongation. *Mol. Cell* **30,** 557–566
13. Koyama, H., Ueda, T., Ito, T., and Sekimizu, K. (2010) Novel RNA polymerase II mutation suppresses transcriptional fidelity and oxidative stress sensitivity in rpb9Delta yeast. *Genes Cells* **15,** 151–159
14. Holmes, S. F., Santangelo, T. J., Cunningham, C. K., Roberts, J. W., and Erie, D. A. (2006) Kinetic investigation of *Escherichia coli* RNA polymerase mutants that influence nucleotide discrimination and transcription fidelity. *J. Biol. Chem.* **281,** 18677–18683
15. Svetlov, V., Vassylyev, D. G., and Artsimovitch, I. (2004) Discrimination against deoxyribonucleotide substrates by bacterial RNA polymerase. *J. Biol. Chem.* **279,** 38087–38090
16. Gordon, A. J., Halliday, J. A., Blankschien, M. D., Burns, P. A., Yatagai, F., and Herman, C. (2009) Transcriptional infidelity promotes heritable phenotypic change in a bistable gene network. *PLoS Biol.* **7,** e44
17. Ba, Y., Tonoki, H., Tada, M., Nakata, D., Hamada, J., and Moriuchi, T. (2000) Transcriptional slippage of p53 gene enhanced by cellular damage in rat liver. Monitoring the slippage by a yeast functional assay. *Mutat. Res.* **447,** 209–220
18. Baranov, P. V., Hammer, A. W., Zhou, J., Gesteland, R. F., and Atkins, J. F. (2005) Transcriptional slippage in bacteria. Distribution in sequenced genomes and utilization in IS element gene expression. *Genome Biol.* **6,** R25
19. Anikin, M., Molodtsov, D., Temiakov, D., and McAllister. (2010) Transcript Slippage and Recoding, in *Recoding: Expansion of Decoding Rules Enriches Gene Expression* (J. F. Atkins & Raymond F. Gesteland, eds) pp. 409–434, Springer, New York
20. Penno, C., Hachani, A., Biskri, L., Sansonetti, P., Allaoui, A., and Parsot, C. (2006) Transcriptional slippage controls production of type III secretion apparatus components in *Shigella flexneri*. *Mol. Microbiol.* **62,** 1460–1468
21. Ratinier, M., Boulant, S., Combet, C., Targett-Adams, P., McLauchlan, J., and Lavergne, J. P. (2008) Transcriptional slippage prompts recoding in alternate reading frames in the hepatitis C virus (HCV) core sequence from strain HCV-1. *J. Gen. Virol.* **89,** 1569–1578
22. Linton, M. F., Raabe, M., Pierotti, V., and Young, S. G. (1997) Reading-frame restoration by transcriptional slippage at long stretches of adenine residues in mammalian cells. *J. Biol. Chem.* **272,** 14127–14132
23. van Leeuwen, F. W., Kros, J. M., Kamphorst, W., van Schravendijk, C., and de Vos, R. A. (2006) Molecular misreading. The occurrence of frameshift proteins in different diseases. *Biochem. Soc. Trans.* **34,** 738–742
24. van Leeuwen, F. W., Fischer, D. F., Benne, R., and Hol, E. M. (2000) Molecular misreading. A new type of transcript mutation in gerontology. *Ann. N.Y. Acad. Sci.* **908,** 267–281
25. Turnbough, C. L., Jr. (2008) Regulation of bacterial gene expression by the NTP substrates of transcription initiation. *Mol. Microbiol.* **69,** 10–14
26. Turnbough, C. L., Jr., and Switzer, R. L. (2008) Regulation of pyrimidine biosynthetic gene expression in bacteria. Repression without repressors. *Microbiol Mol. Biol. Rev.* **72,** 266–300
27. Wagner, L. A., Weiss, R. B., Driscoll, R., Dunn, D. S., and Gesteland, R. F. (1990) Transcriptional slippage occurs during elongation at runs of adenine or thymine in *Escherichia coli*. *Nucleic Acids Res.* **18,** 3529–3535
28. van Leeuwen, F. W., de Kleijn, D. P., van den Hurk, H. H., Neubauer, A., Sonnemans, M. A., Sluijs, J. A., Köycü, S., Ramdjielal, R. D., Salehi, A., Martens, G. J., Grosveld, F. G., Peter, J., Burbach, H., and Hol, E. M. (1998) Frameshift mutants of $\beta$ amyloid precursor protein and ubiquitin-B in Alzheimer's and Down patients. *Science* **279,** 242–247
29. Raabe, M., Linton, M. F., and Young, S. G. (1998) Long runs of adenines and human mutations. *Am. J. Med. Genet.* **76,** 101–102
30. van Leeuwen, F. W., Fischer, D. F., Kamel, D., Sluijs, J. A., Sonnemans, M. A., Benne, R., Swaab, D. F., Salehi, A., and Hol, E. M. (2000) Molecular misreading. A new type of transcript mutation expressed during aging. *Neurobiol. Aging* **21,** 879–891
31. van Leeuwen, F. W., van Tijn, P., Sonnemans, M. A., Hobo, B., Mann, D. M., Van Broeckhoven, C., Kumar-Singh, S., Cras, P., Leuba, G., Savioz, A., Maat-Schieman, M. L., Yamaguchi, H., Kros, J. M., Kamphorst, W., Hol, E. M., de Vos, R. A., and Fischer, D. F. (2006) Frameshift proteins in autosomal dominant forms of Alzheimer disease and other tauopathies. *Neurology* **66,** S86–92
32. Liu, C., Heath, L. S., and Turnbough, C. L., Jr. (1994) Regulation of pyrBI operon expression in *Escherichia coli* by UTP-sensitive reiterative RNA synthesis during transcriptional initiation. *Genes Dev.* **8,** 2904–2912
33. Jin, D. J. (1994) Slippage synthesis at the galP2 promoter of *Escherichia coli* and its regulation by UTP concentration and cAMP·cAMP receptor protein. *J. Biol. Chem.* **269,** 17221–17227
34. de Vries, N., Duinsbergen, D., Kuipers, E. J., Pot, R. G., Wiesenekker, P., Penn, C. W., van Vliet, A. H., Vandenbroucke-Grauls, C. M., and Kusters, J. G. (2002) Transcriptional phase variation of a type III restriction-modification system in *Helicobacter pylori*. *J. Bacteriol.* **184,** 6615–6623
35. Larsen, B., Wills, N. M., Nelson, C., Atkins, J. F., and Gesteland, R. F. (2000) Nonlinearity in genetic decoding. Homologous DNA replicase genes use alternatives of transcriptional slippage or translational frameshifting. *Proc. Natl. Acad. Sci. U.S.A.* **97,** 1683–1688

36. Penno, C., Sansonetti, P., and Parsot, C. (2005) Frameshifting by transcriptional slippage is involved in production of MxiE, the transcription activator regulated by the activity of the type III secretion apparatus in *Shigella flexneri*. *Mol. Microbiol.* **56,** 204–214
37. Jin, D. J., and Turnbough, C. L., Jr. (1994) An *Escherichia coli* RNA polymerase defective in transcription due to its overproduction of abortive initiation products. *J. Mol. Biol.* **236,** 72–80
38. Jin, D. J. (1996) A mutant RNA polymerase reveals a kinetic mechanisms for the switch between nonproductive stuttering synthesis and productive initiation during promoter clearance. *J. Biol. Chem.* **271,** 11659–11667
39. Strathern, J. N., Malagon, F., Irvin, J., Gotte, D., Shafer, B., Kireeva, M., Lubkowska, L., Jin, D. J., and Kashlev, M. (2013) *J. Biol. Chem.* **288,** 2689–2699
40. Sambrook, J., Fritsch, E. F., and Maniatis, T. (1989) *Molecular Cloning: A Laboratory Manual*, Cold Spring Harbor Laboratory, Cold Spring Harbor, NY
41. Miller, J. H. (1972) *Experiments in Molecular Genetics*, Cold Spring Harbor Laboratory, Plainview, NY
42. Sawitzke, J. A., Thomason, L. C., Costantino, N., Bubunenko, M., Datta, S., and Court, D. L. (2007) Recombineering. *In vivo* genetic engineering in *E. coli*, *S. enterica*, and beyond. *Methods Enzymol.* **421,** 171–199
43. Sawitzke, J. A., Costantino, N., Li, X. T., Thomason, L. C., Bubunenko, M., Court, C., and Court, D. L. (2011) Probing cellular processes with oligo-mediated recombination and using the knowledge gained to optimize recombineering. *J. Mol. Biol.* **407,** 45–59
44. Svenningsen, S. L., Costantino, N., Court, D. L., and Adhya, S. (2005) On the role of Cro in lambda prophage induction. *Proc. Natl. Acad. Sci. U.S.A.* **102,** 4465–4469
45. Alton, N. K., and Vapnek, D. (1979) Nucleotide sequence analysis of the chloramphenicol resistance transposon Tn9. *Nature* **282,** 864–869
46. Datta, S., Costantino, N., and Court, D. L. (2006) A set of recombineering plasmids for gram-negative bacteria. *Gene* **379,** 109–115
47. Zalenskaya, K., Lee, J., Gujuluva, C. N., Shin, Y. K., Slutsky, M., and Goldfarb, A. (1990) Recombinant RNA polymerase. Inducible overexpression, purification and assembly of *Escherichia coli* rpo gene products. *Gene* **89,** 7–12
48. Jin, D. J., and Gross, C. A. (1988) Mapping and sequencing of mutations in the *Escherichia coli* rpoB gene that lead to rifampicin resistance. *J. Mol. Biol.* **202,** 45–58
49. Kireeva, M. L., Lubkowska, L., Komissarova, N., and Kashlev, M. (2003) Assays and affinity purification of biotinylated and nonbiotinylated forms of double-tagged core RNA polymerase II from *Saccharomyces cerevisiae*. *Methods Enzymol.* **370,** 138–155
50. Kireeva, M. L., and Kashlev, M. (2009) Mechanism of sequence-specific pausing of bacterial RNA polymerase. *Proc. Natl. Acad. Sci. U.S.A.* **106,** 8900–8905
51. Jin, D. J., and Gross, C. A. (1989) Characterization of the pleiotropic phenotypes of rifampin-resistant rpoB mutants of *Escherichia coli*. *J. Bacteriol.* **171,** 5229–5231
52. Garibyan, L., Huang, T., Kim, M., Wolff, E., Nguyen, A., Nguyen, T., Diep, A., Hu, K., Iverson, A., Yang, H., and Miller, J. H. (2003) Use of the rpoB gene to determine the specificity of base substitution mutations on the *Escherichia coli* chromosome. *DNA Repair* **2,** 593–608
53. Lisitsyn, N. A., Sverdlov, E. D., Moiseyeva, E. P., Danilevskaya, O. N., and Nikiforov, V. G. (1984) Mutation to rifampicin resistance at the beginning of the RNA polymerase beta subunit gene in *Escherichia coli*. *Mol. Gen. Genet.* **196,** 173–174
54. Thomason, L., Court, D. L., Bubunenko, M., Costantino, N., Wilson, H., Datta, S., and Oppenheim, A. (2007) *Current Protocols in Molecular Biology* (Ausubel, F. M., Brent, R., Kingston, R. E., Moore, D. D., Seidman, J. G., Smith, J. A., and Struhl, K., eds) Chapter 1, Unit 1.16
55. Kireeva, M., Nedialkov, Y. A., Gong, X. Q., Zhang, C., Xiong, Y., Moon, W., Burton, Z. F., and Kashlev, M. (2009) Millisecond phase kinetic analysis of elongation catalyzed by human, yeast, and *Escherichia coli* RNA polymerase. *Methods* **48,** 333–345
56. Samkurashvili, I., and Luse, D. S. (1996) Translocation and transcriptional arrest during transcript elongation by RNA polymerase II. *J. Biol. Chem.* **271,** 23495–23505
57. Komissarova, N., Becker, J., Solter, S., Kireeva, M., and Kashlev, M. (2002) Shortening of RNA:DNA hybrid in the elongation complex of RNA polymerase is a prerequisite for transcription termination. *Mol. Cell* **10,** 1151–1162
58. Jin, D. J., and Gross, C. A. (1991) RpoB8, a rifampicin-resistant termination-proficient RNA polymerase, has an increased Km for purine nucleotides during transcription elongation. *J. Biol. Chem.* **266,** 14478–14485
59. Vassylyev, D. G., Sekine, S., Laptenko, O., Lee, J., Vassylyeva, M. N., Borukhov, S., and Yokoyama, S. (2002) Crystal structure of a bacterial RNA polymerase holoenzyme at 2.6 A resolution. *Nature* **417,** 712–719
60. Atkins, J. F., and Björk, G. R. (2009) A gripping tale of ribosomal frameshifting. Extragenic suppressors of frameshift mutations spotlight P-site realignment. *Microbiol. Mol. Biol. Rev.* **73,** 178–210
61. Chakrabarti, S. L., and Gorini, L. (1977) Interaction between mutations of ribosomes and RNA polymerase. A pair of strA and rif mutants individually temperature-insensitive but temperature-sensitive in combination. *Proc. Natl. Acad. Sci. U.S.A.* **74,** 1157–1161